



Ministry of Science, Research & Technology
Iranian Research Organization for
Science and Technology (IROST)

Research paper

Application of $\text{Fe}_3\text{O}_4@\text{THAM-CH}_2\text{CH}_2\text{Cl}$ magnetic nanoparticle as a new adsorbent in ultrasonically assisted removal of Congo red from aqueous solutions

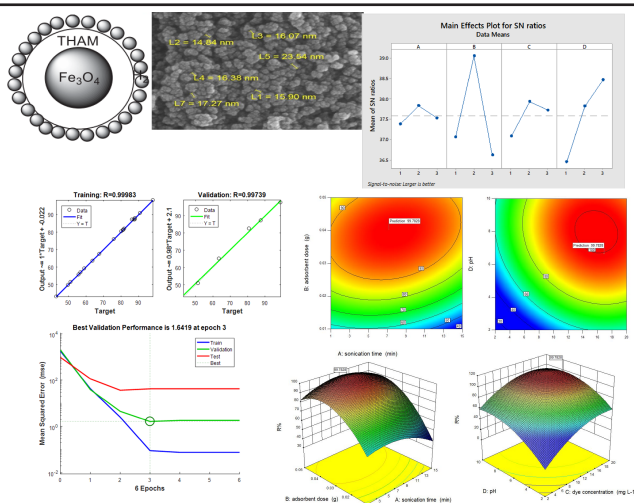
Reyhaneh Mokari, Mashaallah Rahmani*

Department of Chemistry, Faculty of Science, University of Sistan and Baluchestan, Zahedan, Iran

HIGHLIGHTS

- $\text{Fe}_3\text{O}_4 @ \text{THAM} - \text{CH}_2\text{CH}_2\text{Cl}$ magnetic nanoparticle (as a new adsorbent) was applied to remove dye pollutant in an aqueous environment.
- To increase the adsorption efficiency, Taguchi, RSM, and ANN methods were used to investigate, improve, optimize, and model important operational parameters in ultrasonic adsorption.
- The kinetic, isotherm, and thermodynamic for the proposed method were assayed.

GRAPHICAL ABSTRACT



ARTICLE INFO

Article history:

Received 28 February 2023

Revised 7 May 2023

Accepted 9 May 2023

Keywords:

Congo red
 $\text{Fe}_3\text{O}_4@\text{THAM-CH}_2\text{CH}_2\text{Cl}$
Multivariate methods
Wastewater

DOI: [10.22104/JPST.2023.6153.1223](https://doi.org/10.22104/JPST.2023.6153.1223)



This is an open access article under the CC-BY 4.0 license (<http://creativecommons.org/licenses/by/4.0/>).

ABSTRACT

The objective of this work was to evaluate the efficiency of a promising ultrasonically assisted adsorption with the $\text{Fe}_3\text{O}_4@\text{THAM-CH}_2\text{CH}_2\text{Cl}$ magnetic nanoparticle (MNPS) as a new adsorbent for the elimination of Congo red from water samples. The FE-SEM images show that $\text{Fe}_3\text{O}_4@\text{THAM-CH}_2\text{CH}_2\text{Cl}$ MNPs adsorbent is spherical. Due to the presence of pores on the $\text{Fe}_3\text{O}_4@\text{THAM-CH}_2\text{CH}_2\text{Cl}$ MNPs adsorbent surface, the proposed adsorbent can remove Congo red from the aqueous environment by trapping the pollutant in its pores. Different parameters influencing the ultrasonically assisted adsorption (UAA) by the $\text{Fe}_3\text{O}_4@\text{THAM-CH}_2\text{CH}_2\text{Cl}$ MNPs adsorbent, including the dye concentration and adsorbent mass, ultrasonic time, and pH, were studied and optimized by multivariate methods. The best adsorption efficiency was obtained at 0.04 g of adsorbent, 17 mg.L^{-1} of dye, pH = 6.6, and ultrasonic treatment for 7.2 min. The results indicated that the efficiency of dye adsorption ranged from 97.85 to 99.65 %. The kinetic, isotherm, and thermodynamic for the proposed method were assayed. The larger R^2 for the pseudo-second kinetic model indicates that this model is more suitable to describe the adsorption process of Congo red on the $\text{Fe}_3\text{O}_4@\text{THAM-CH}_2\text{CH}_2\text{Cl}$ MNPs adsorbent. The Langmuir adsorption isotherm had a larger correlation coefficient ($R^2 = 0.9987$), which indicates it fits best with the experimental data and is more suitable for the Congo red adsorption process. Analysis of actual samples showed that Congo red removal values (R %, mean \pm standard deviation, $n = 3$) in tap water and wastewater were 98.48 ± 1.52 % and 98.05 ± 2.11 %, respectively.

1. Introduction

Dyes from industries are one of the most critical pollutants in water and wastewater [1-3]. Water pollution caused by various human biological, agricultural, and industrial activities as well as excessive exploitation of limited water resources, will lead to a water crisis in the coming years [4-6]. For instance, most textile industries do not treat wastewater properly [7]. Congo red (CR), an anionic azo dye based on benzidine and soluble in water, is metabolized to benzidine, which threatens human health [8]. This substance is widely applied in the manufacture of plastic, rubber, paper, and textile. Since this substance is a skin and eye irritant and causes respiratory problems, nausea, vomiting, allergic reactions, and obvious carcinogenesis in humans, it should be removed from water resources. The chemical structure of CR dye is shown in Fig. S1 ([Supplementary File](#)).

Various methods, such as advanced reverse osmosis [9], ultrafiltration [10], oxidation [11], ion exchange [12], and visible-light irradiation [13], are used to monitor dye contamination. All these techniques have disadvantages, such as high costs, sludge production, and complexity of the treatment process. However, despite the existence of many methods, adsorption has become one of the most popular methods used to remove contaminants in sample solutions due to its simple techniques, lower price, and high efficiency [14-16]. Different adsorbents have been used to eliminate pollutants from water samples [17-19]. However, new adsorbents with higher removal capacity are more economical and are experiencing growing interest from researchers [20-22]. Numerous factors, such as the concentration of dye, mass of adsorbent, time, and pH, affect the examination of the adsorption process [23, 24]. Also, the use of absorption columns to treat colored wastewater may allow some adsorbents into the environment through the treated wastewater, leading to severe problems (in particular nanomaterials), which defeats the purpose of treating colored wastewater.

Recently, Fe_3O_4 magnetic nanoparticles have been used as an intermediate in the synthesis of magnetic nanoparticle catalysts [25], and the use of magnetic nanomaterial is becoming a growing interest for the removal of various pollutants [26]. Adsorbents must be regenerated after use to maintain absorption efficiency, although adsorbent MNPs can collect NPs through a magnetic field [27]. The Fe_3O_4 adsorbent is the most

common magnetic core used in adsorption studies; however, to achieve a higher adsorption capacity, it must be functionally coated to prevent oxidation. Oxidation leads to damage to the magnetic properties, reduction of its absorption capacity, and limits its use. Therefore, to compensate for these limitations, several studies have focused on the surface functionalization of MNPs. In this research, surface functionalization of Fe_3O_4 MNPs is accomplished using THAM or tris (hydroxymethyl) aminomethane, which produces a suitable functionalized surface and results in chemical stability for Fe_3O_4 MNPs. THAM is rich in donor-acceptor groups, which makes it useful for the surface functionalization of Fe_3O_4 MNPs, improving its stability and preventing oxidation. Therefore, an MNPs adsorbent in a created magnetic field can be used to separate particles from treated wastewater [28]. Nowadays, one of the main research objectives is economic optimization. Classical methods of changing one variable at a time take a long time; they require many experiments and cannot show the interactive effects of variables. Furthermore, the optimized conditions in classical methods are not always reliable [29]. Conversely, the optimization of parameters in the implementation of processes with the help of multivariate methods is being reported in many research fields [30]. Experimental methods such as Taguchi, response surface methodology (RSM), and artificial neural networks (ANN) enable researchers to rationally reduce the number of experiments, reduce costs, and generate more research benefits [31].

Herein, we first developed a new MNP, Fe_3O_4 MNPs adsorbent combined with THAM ($\text{Fe}_3\text{O}_4@\text{THAM-CH}_2\text{CH}_2\text{Cl}$ MNPs adsorbent), with improved adsorption capacity, stability, and recyclability for removal of CR from the aqueous environment. Then, Taguchi, RSM, and ANN methods were used to investigate, improve, optimize, and model important operational parameters in ultrasonic adsorption. Finally, the application of the dye removal method in water and wastewater samples was investigated.

2. Experimental

The synthesis of $\text{Fe}_3\text{O}_4@\text{THAM}$ MNPs is included in the [supplementary information](#). The FE-SEM image of $\text{Fe}_3\text{O}_4@\text{THAM-CH}_2\text{CH}_2\text{Cl}$ shows that the nanoparticles are spherical (Fig. S2, [Supplementary File](#)). The BET measurements confirmed a specific

surface area of 121.79 m².g⁻¹, a total pore volume of 27.9 cm³.g⁻¹, and a mean pore size of 8.14 nm. The presence of pores on the Fe₃O₄@THAM MNPs surface allows the proposed adsorbent to trap the pollutant, removing Congo red from the aqueous environment. To investigate the adsorption process, 0.01 - 0.05 g of Fe₃O₄@THAM-CH₂CH₂Cl adsorbent was added to a sample solution (pH = 2-10) containing Congo red with an appropriate concentration (2-20 mg.L⁻¹). This mixture was vigorously shaken using an ultrasonic system for different time intervals (1-15 min). At the end of the decolorization process, the residual Congo red was determined by a spectrophotometer (2120 UV plus, Optizen) at 500 nm.

2.1. Taguchi method

In this study, the Taguchi design was utilized to assess the impact of each parameter on the removal of CR by the Fe₃O₄@THAM-CH₂CH₂Cl MNPs adsorbent and to search for an optimal parametric combination to access the proper surface. After performing nine experiments using the Taguchi method, the removal process results were assayed to identify the optimal conditions for the removal of dye using the Fe₃O₄@THAM-CH₂CH₂Cl MNPs adsorbent. In the Taguchi model, we use a converted response function shown as an *S/N* ratio for accurate analysis. This formula is calculated as Eq. (1):

$$\frac{S}{N} = -10 \log \frac{(\frac{1}{y_1^2} + \frac{1}{y_2^2} + \dots + \frac{1}{y_n^2})}{n} \quad (1)$$

where y_n is the measured value for each step of the adsorption process, S is the measured response value for each experiment in each test, and n denotes the number of times the experiment was repeated. Using the Taguchi method, the effects of independent variables can be investigated. The design of experimental runs for the proposed Taguchi method by *S/N* ratios (Data Means) for each level of variables is shown in Table 1. The parameters are entered as coded and uncoded. The Taguchi method's optimal values were employed as a preliminary implementation of the Central Composite Design (CCD) for removing Congo red with the Fe₃O₄@THAM-CH₂CH₂Cl adsorbent.

2.2. Response Surface Methodology (RSM) Modeling

Optimizing the effective parameters influencing the ultrasonically assisted adsorption by Fe₃O₄@THAM-CH₂CH₂Cl adsorbent is essential. RSM is a useful technique for process optimization where the response is influenced by several variables, and the objective is to optimize the response. In this study, the adsorption process was investigated by carrying out the 30 experiments proposed by CCD (a type of RSM), and the results were entered into the software to evaluate the optimized conditions to remove Congo red using the proposed adsorbent.

The response model may be expressed as Eq. (2):

$$Y = b_0 + \sum_{i=1}^4 b_i x_i + \sum_{i=1}^4 b_{ii} x_i^2 + \sum_{i=1}^3 \sum_{j=i+1}^4 b_{ij} x_i x_j \quad (2)$$

Table 1. The design of experimental runs of Taguchi method for the removal of Congo red (The parameters are entered in both coded and uncoded ways)

| Run | Factor 1 (A: Ultrasonic time, min) | | Factor 2 (B: Mass of adsorbent, g) | | Factor 3 (C: Concentration of dye, mg.L ⁻¹) | | Factor 4 (D: pH) | | S/N ratio |
|-----|---------------------------------------|---------|---------------------------------------|---------|--|---------|---------------------|---------|-----------|
| | Coded | Uncoded | Coded | Uncoded | Coded | Uncoded | Coded | Uncoded | |
| 1 | 1 | 4 | 1 | 0.01 | 1 | 5 | 1 | 2 | 35.24 |
| 2 | 1 | 4 | 2 | 0.03 | 2 | 11 | 2 | 4 | 39.45 |
| 3 | 1 | 4 | 3 | 0.06 | 3 | 17 | 3 | 6 | 37.45 |
| 4 | 2 | 8 | 1 | 0.01 | 2 | 11 | 3 | 6 | 38.55 |
| 5 | 2 | 8 | 2 | 0.03 | 3 | 17 | 1 | 2 | 38.31 |
| 6 | 2 | 8 | 3 | 0.06 | 1 | 5 | 2 | 4 | 36.61 |
| 7 | 3 | 12 | 1 | 0.01 | 3 | 17 | 2 | 4 | 37.39 |
| 8 | 3 | 12 | 2 | 0.03 | 1 | 5 | 3 | 6 | 39.41 |
| 9 | 3 | 12 | 3 | 0.06 | 2 | 11 | 1 | 2 | 35.79 |

In this equation, b_i is the linear coefficient, b_{ii} is the quadratic coefficient, b_{ij} is the interaction coefficient, x_i and x_j are the encoded values of the process variables, Y is the predicted data, and b_0 is the constant coefficient [32].

3. Results and discussion

3.1. Taguchi optimization

The Taguchi method uses a response function for mathematical analysis and more accurate results, defined as the S/N ratio. The optimization by the proposed model is confirmed using experiments conducted after finding the levels based on the S/N ratio (Data Means) for each level of variables. In the removal process, ultrasonic action increases the mass transfer of adsorption processes. So, the removal process increased as the ultrasonic time increased. At lower pH, the adsorbent surface is more positively charged, indicating that the adsorption of CR from aqueous solutions is favorable.

According to the results of the main effects plot for SN ratios, the optimized conditions for the removal of CR by $\text{Fe}_3\text{O}_4@\text{THAM-CH}_2\text{CH}_2\text{Cl}$ adsorbent occurred in an ultrasonic time of 8 min, adsorbent amount of 0.03 g, dye concentration of 11 mg.L^{-1} , and pH = 6 (Fig. 1). The Taguchi method's optimal values were employed as a preliminary implementation of the RSM-CCD design for the removal of Congo red by $\text{Fe}_3\text{O}_4@\text{THAM-CH}_2\text{CH}_2\text{Cl}$ adsorbent.

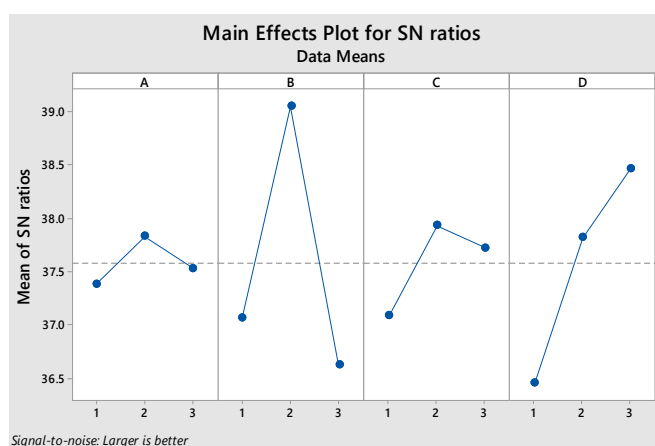


Fig. 1. Main Effects Plot for SN ratios (Data Means) for (A) ultrasonic time (A), adsorbent amount (B), dye concentration (C) and pH of the solution (D) on the removal of Congo red by $\text{Fe}_3\text{O}_4@\text{THAM-CH}_2\text{CH}_2\text{Cl}$ adsorbent.

3.2. RSM Model

To investigate the adsorption process, the results of 30 experiments proposed by CCD, a type of RSM, were assayed to measure the optimal conditions for the ultrasonically assisted adsorption (UAA) removal of CR with the proposed $\text{Fe}_3\text{O}_4@\text{THAM-CH}_2\text{CH}_2\text{Cl}$ adsorbent. Using this model, we first determined the effects of variables on the response. Then, the effects of the independent variables were investigated. Table 2 shows the design of the experimental runs for the proposed RSM-CCD model. Based on the results (Figs. 2(a)-(d)), the reasonable agreement of experimental and predicted values indicates the high efficiency of the mentioned equation in evaluating the experimental data. Also, the data were assayed to check for normal residues. Based on the results (Fig. 2(a)), the points are close to the straight line, which indicates that the errors are normally and independently distributed. According to Fig. 2(c), the correlation between the predicted and experimental values indicates the model's suitability to accurately represent the UAA removal of Congo red by the proposed $\text{Fe}_3\text{O}_4@\text{THAM-CH}_2\text{CH}_2\text{Cl}$ adsorbent. Based on the results (Fig. 2(d)), the remaining stochastic pattern and the data have a normal distribution, indicating the method's adequacy and that the quadratic model is suitable to indicate the removal of CR dye by $\text{Fe}_3\text{O}_4@\text{THAM-CH}_2\text{CH}_2\text{Cl}$ MNPs adsorbent.

According to the RSM-CCD method, the adequacy of the model was further tested by ANOVA (analysis of variance) (Table 3). The results showed that this model could significantly remove dye by the proposed method using $\text{Fe}_3\text{O}_4@\text{THAM-CH}_2\text{CH}_2\text{Cl}$ MNPs adsorbent. The fit between the experimental values versus predicted data was assayed by determining the significance of the coefficients' P -value and F -value. According to Table 3, the R^2 , $\text{Adj-}R^2$, and $\text{Pred-}R^2$ values were 0.9978, 0.9958, and 0.9884, respectively (P -value < 0.0001 is considered significant). Also, the F -value for the model was 492.79, which indicates the model's high value of this model, with only 0.01 % of the F -value high value being related to noise. Also, the low data (less than 0.05) of the P -value confirm this. Given that the F -value Lack of fit (4.59) value is slightly smaller than the Pure Error, the model is meaningful. Based on the ANOVA results, the quadratic model is suitable to remove dye by $\text{Fe}_3\text{O}_4@\text{THAM-CH}_2\text{CH}_2\text{Cl}$ MNPs adsorbent. According to Table 3, the P -values of AC and BC (P =

Table 2. The design of experimental runs of RSM-CCD model for the removal of Congo red by UAA proposed by $\text{Fe}_3\text{O}_4@\text{THAM-CH}_2\text{CH}_2\text{Cl}$ adsorbent and ANN predicted.

| Run | A: Ultrasonic time (min) | B: Mass of adsorbent (g) | C: Concentration of dye (mg.L ⁻¹) | D: pH | RSM | | ANN Predicted |
|-----|-----------------------------|-----------------------------|--|-------|----------|-----------|------------------|
| | | | | | Measured | Predicted | |
| 1 | 4.5 | 0.04 | 6.5 | 8 | 80.17 | 80.87 | 80.36 |
| 2 | 11.5 | 0.02 | 6.5 | 8 | 55.82 | 57.49 | 55.65 |
| 3 | 11.5 | 0.04 | 6.5 | 8 | 80.84 | 80.08 | 82.51 |
| 4 | 4.5 | 0.02 | 6.5 | 8 | 63.76 | 64.05 | 63.48 |
| 5 | 8 | 0.03 | 11 | 6 | 87.52 | 87.38 | 87.13 |
| 6 | 4.5 | 0.02 | 15.5 | 4 | 67.65 | 68.17 | 67.46 |
| 7 | 8 | 0.03 | 20 | 6 | 90.85 | 90.54 | 90.83 |
| 8 | 11.5 | 0.02 | 15.5 | 8 | 75.92 | 75.38 | 75.91 |
| 9 | 4.5 | 0.04 | 6.5 | 4 | 56.90 | 57.20 | 56.89 |
| 10 | 8 | 0.03 | 11 | 10 | 87.99 | 86.70 | 87.98 |
| 11 | 11.5 | 0.02 | 15.5 | 4 | 63.50 | 63.95 | 65.13 |
| 12 | 1 | 0.03 | 11 | 6 | 81.33 | 79.84 | 81.32 |
| 13 | 11.5 | 0.04 | 15.5 | 8 | 98.20 | 98.54 | 98.17 |
| 14 | 4.5 | 0.04 | 15.5 | 8 | 99.01 | 100.05 | 97.56 |
| 15 | 8 | 0.03 | 11 | 6 | 87.78 | 87.38 | 87.13 |
| 16 | 8 | 0.03 | 11 | 2 | 51.22 | 51.60 | 51.32 |
| 17 | 8 | 0.03 | 11 | 6 | 87.21 | 87.38 | 87.13 |
| 18 | 11.5 | 0.04 | 6.5 | 4 | 59.05 | 59.45 | 59.11 |
| 19 | 4.5 | 0.02 | 6.5 | 4 | 44.47 | 45.28 | 54.93 |
| 20 | 11.5 | 0.04 | 15.5 | 4 | 82.74 | 82.21 | 86.91 |
| 21 | 8 | 0.01 | 11 | 6 | 51.44 | 50.56 | 50.81 |
| 22 | 8 | 0.03 | 2 | 6 | 49.79 | 49.19 | 49.66 |
| 23 | 4.5 | 0.02 | 15.5 | 8 | 81.88 | 82.64 | 81.88 |
| 24 | 11.5 | 0.02 | 6.5 | 4 | 43.06 | 41.78 | 43.05 |
| 25 | 8 | 0.05 | 11 | 6 | 85.67 | 85.64 | 82.01 |
| 26 | 15 | 0.03 | 11 | 6 | 74.24 | 74.82 | 65.89 |
| 27 | 4.5 | 0.04 | 15.5 | 4 | 81.18 | 80.67 | 81.15 |
| 28 | 8 | 0.03 | 11 | 6 | 86.29 | 87.38 | 87.13 |
| 29 | 8 | 0.03 | 11 | 6 | 87.64 | 87.38 | 87.13 |
| 30 | 8 | 0.03 | 11 | 6 | 87.82 | 87.38 | 87.13 |

0.5148, 0.5909, respectively) in the CCD model are not significant. Therefore, these two-way interactions were removed from Eq. (3). Using the obtained data, the final model to remove dye by the proposed method can be described using the equation below.

$$Y (\% \text{ Removal}) = -103.41914 + 2.46525 \times A + 3035.44444 \times B + 7.76182 \times C + 18.39710 \times D + 41.12500 \times A \times B - 0.10884 \times A \times D + 61.40625 \times B \times D - 0.11924 \times C \times D - 0.20503 \times A^2 - 48190.62500 \times B^2 - 0.21619 \times C^2 - 1.13914 \times D^2 \quad (3)$$

3.3. Effects of parameters

Interactive variables were assayed by counter and response surface plots to assess the parameters' influence in removing Congo red by $\text{Fe}_3\text{O}_4@\text{THAM-CH}_2\text{CH}_2\text{Cl}$ adsorbent. These plots were used to determine the removal of Congo red dye over interactive variables: the dye concentration, the adsorbent mass, ultrasonic time, and pH of the solution (Figs. 3(a) and 3(b)). According to Fig. 3(a), the $\text{Fe}_3\text{O}_4@\text{THAM-CH}_2\text{CH}_2\text{Cl}$

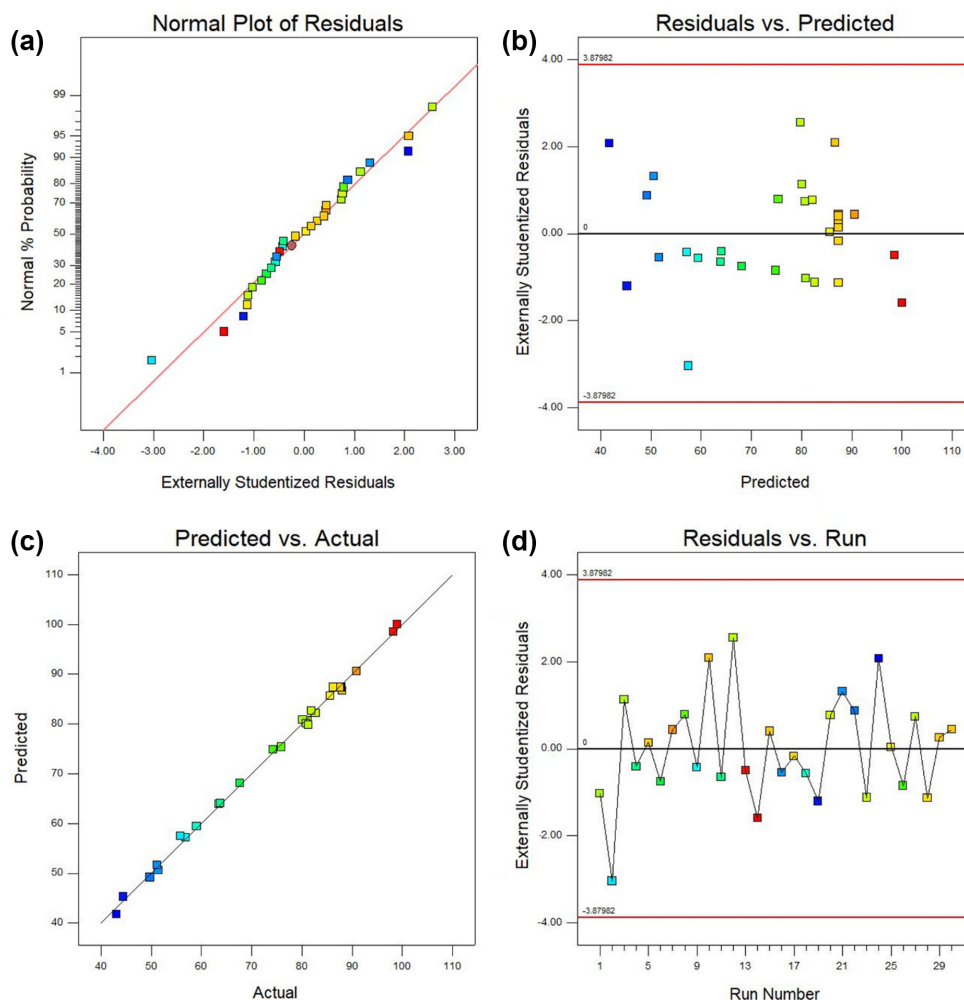


Fig. 2. Normal probability plots of residuals (a) plot of residuals versus predicted values (b) experimental versus predicted values (c) plot of residuals versus run number (d) for the removal of Congo red by UAA proposed by $\text{Fe}_3\text{O}_4@\text{THAM-CH}_2\text{CH}_2\text{Cl}$ adsorbent.

adsorbent's adsorption efficiency of Congo red dye increased as the adsorbent mass increased, due to a corresponding increase in the number of available sites for the interaction of Congo red with MNPs adsorbent; therefore, the adsorption efficiency of Congo red from the solution increased. However, at more than 0.04 g of $\text{Fe}_3\text{O}_4@\text{THAM-CH}_2\text{CH}_2\text{Cl}$ adsorbent, the Congo red removal efficiency ceases to increase significantly and remains relatively constant. According to Fig. 3(b), the $\text{Fe}_3\text{O}_4@\text{THAM-CH}_2\text{CH}_2\text{Cl}$ adsorbent in 17 mg.L^{-1} of dye obtained the best adsorption efficiency of Congo red because, at low concentrations, the number of active adsorbent sites is very high. Thus, the adsorption efficiency of Congo red by $\text{Fe}_3\text{O}_4@\text{THAM-CH}_2\text{CH}_2\text{Cl}$ adsorbent increases as the dye concentration increases up to 17 mg.L^{-1} of dye, where it remains constant. Ultrasonic action enhances the mass transfer of the sorption processes. Therefore, it can potentially influence the removal process (Fig. 3(a)). As can be seen

in the figure, the adsorption efficiency of Congo red by $\text{Fe}_3\text{O}_4@\text{THAM-CH}_2\text{CH}_2\text{Cl}$ adsorbent was increased as the ultrasonic time increased. However, above 7.2 min (after equilibrium), the Congo red removal efficiency no longer increased significantly, remaining relatively constant. The pH can affect the elimination of material due to its effect on site dissociation of the adsorbent and hydrolysis of species. At a lower pH, the adsorbent surface has a more positive charge. Based on Fig. 3(b), the highest removal efficiency occurs at $\text{pH} = 6.6$. This is due to the MNP adsorbent surface having a positive charge. On the other hand, the sulphonate group in Congo red is negatively charged, indicating that the elimination of Congo red dye from water samples was unfavorable due to the electrostatic repulsion. It should be noted that the possibility of predicting the data was assayed under optimal conditions. Based on the results (Table 4), the adsorption efficiencies of CR were in the range of 97.85 to 99.65%.

Table 3. ANOVA for proposed method for the removal of Congo red by UAA proposed by $\text{Fe}_3\text{O}_4@\text{THAM-CH}_2\text{CH}_2\text{Cl}$ adsorbent.

| Source | SS | DF | MS | F-Value | P-Value | |
|---------------------|---------|----|---------|---------|----------|------------|
| Model | 7758.91 | 14 | 554.21 | 492.79 | < 0.0001 | signt. |
| A | 37.68 | 1 | 37.68 | 33.50 | < 0.0001 | |
| B | 1846.09 | 1 | 1846.09 | 1641.51 | < 0.0001 | |
| C | 2565.35 | 1 | 2565.35 | 2281.08 | < 0.0001 | |
| D | 1847.84 | 1 | 1847.84 | 1643.07 | < 0.0001 | |
| AB | 33.15 | 1 | 33.15 | 29.48 | < 0.0001 | |
| AC | 0.50 | 1 | 0.50 | 0.45 | 0.5148 | |
| AD | 9.29 | 1 | 9.29 | 8.26 | 0.0116 | |
| BC | 0.34 | 1 | 0.34 | 0.30 | 0.5909 | |
| BD | 24.13 | 1 | 24.13 | 21.46 | 0.0003 | |
| CD | 18.43 | 1 | 18.43 | 16.38 | 0.0011 | |
| A ² | 173.02 | 1 | 173.02 | 153.85 | < 0.0001 | |
| B ² | 636.98 | 1 | 636.98 | 566.40 | < 0.0001 | |
| C ² | 525.68 | 1 | 525.68 | 467.42 | < 0.0001 | |
| D ² | 569.48 | 1 | 569.48 | 506.37 | < 0.0001 | |
| Residual | 16.87 | 15 | 1.12 | | | |
| Lack of Fit | 15.21 | 10 | 1.52 | 4.59 | 0.0532 | not signt. |
| Pure Error | 1.66 | 5 | 0.33 | | | |
| Cor Total | 7775.78 | 29 | | | | |
| Std. Dev. | 1.06 | | | | | |
| R ² | 0.9978 | | | | | |
| Adj-R ² | 0.9958 | | | | | |
| Pred-R ² | 0.9884 | | | | | |

3.4. Modeling by artificial neural networks (ANN)

The neural network architecture of the ANN model includes input, hidden, and output layers [33]. The software package MATLAB 2016b with Levenberg–Marquardt algorithm was applied to model the removal of Congo red by the proposed UAA of $\text{Fe}_3\text{O}_4@\text{THAM-CH}_2\text{CH}_2\text{Cl}$ MNPs adsorbent. In this study, the experimental runs were used to design the ANN. Variable parameters in the experimental runs include the dye concentration, adsorbent mass, ultrasonic time, and pH of the sample solution. Table 2 gives the output layer values, which indicate the removal efficiency of the target method. The hidden layers, from 2 to 20 layers, were assayed, and their optimized choice is based on the highest R^2 and the lowest MSE (mean

Table 4. Optimum conditions derived by RSM for the proposed UAA by $\text{Fe}_3\text{O}_4@\text{THAM-CH}_2\text{CH}_2\text{Cl}$ adsorbent.

| Test | A* | B | C | pH | Experimental | Predicted |
|------|-----|------|----|-----|--------------|-----------|
| 1 | 7.2 | 0.04 | 17 | 6.6 | 98.43 | 99.78 |
| 2 | 7.2 | 0.04 | 17 | 6.6 | 99.32 | 99.78 |
| 3 | 7.2 | 0.04 | 17 | 6.6 | 97.85 | 99.78 |
| 4 | 7.2 | 0.04 | 17 | 6.6 | 98.25 | 99.78 |
| 5 | 7.2 | 0.04 | 17 | 6.6 | 99.65 | 99.78 |

*A: Ultrasonic time (min), B: Mass of adsorbent (g), C: Concentration of dye (mg.L^{-1}).

square error). Based on the results, the architecture of the artificial neural network is 4-14-1 for the proposed UAA by $\text{Fe}_3\text{O}_4@\text{THAM-CH}_2\text{CH}_2\text{Cl}$ MNPs adsorbent model. Based on the results, the data of MSE and R^2 for the training, validation, and testing dataset are 0.0904, 0.9998, and 1.6419 and 0.9974, 42.0583, and 0.9204, respectively. The correlation coefficients of the graphs between outputs and targets of the ANN model (Fig. 4) and the experimental data are close to one, which indicates the validity of the ANN model to successfully predict the removal of Congo red by $\text{Fe}_3\text{O}_4@\text{THAM-CH}_2\text{CH}_2\text{Cl}$ MNPs adsorbent.

3.5. Kinetic, isotherm, and thermodynamic of adsorption

Characteristics of the pollutants' absorption rate of pollutants were used to assess the kinetics, isotherm, and thermodynamics of the adsorption process [21]. This study evaluated the isotherm, kinetic, and thermodynamic of the adsorption process of CR onto the $\text{Fe}_3\text{O}_4@\text{THAM-CH}_2\text{CH}_2\text{Cl}$ MNPs adsorbent. The larger correlation coefficient ($R^2 = 0.9981$) for the pseudo-second kinetic model indicates that this model is more suitable for describing the process of adsorption of Congo dye on the proposed adsorbent (Table 5).

The isotherm for the adsorption process of Congo red by the proposed adsorbent was also assayed. According to the results (Table S1, [Supplementary File](#)), the Langmuir adsorption isotherm has a larger correlation coefficient ($R^2 = 0.9987$), indicating the best fit with the experimental data, and the proposed adsorbent is more suitable for the Congo red adsorption process, and that the adsorption process could be performed by the proposed method. Lastly, the thermodynamic parameters were investigated at different temperatures (Table 6). According to the

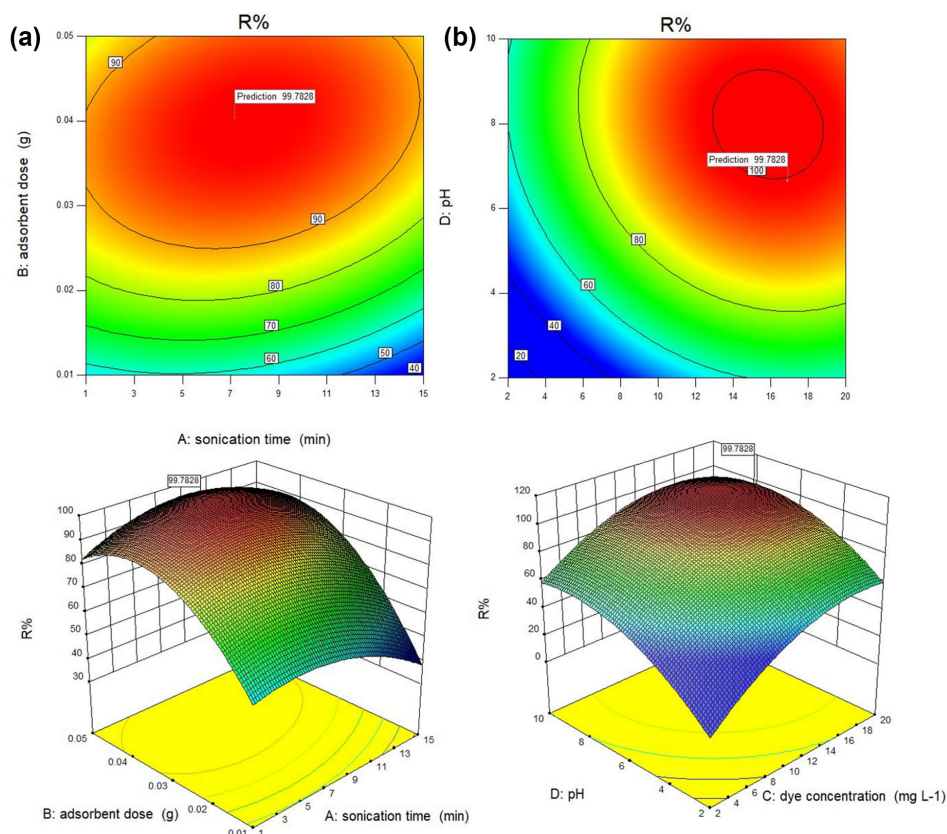


Fig. 3. Contour and response surface plots for (a) ultrasonic time (A) and adsorbent amount (B), (b) dye concentration (C) and pH of the solution (D) on the removal of Congo red by $\text{Fe}_3\text{O}_4@\text{THAM-CH}_2\text{CH}_2\text{Cl}$ adsorbent.

results, the negativity of ΔG° and ΔH° showed that the adsorption process is spontaneous and exothermic.

According to the results (Fig. S3, [Supplementary File](#)), only about a 5% change in adsorbent efficiency is observed after 6 runs of adsorption and desorption. This confirms that the proposed adsorbent can be regenerated and reused.

3.6. Real sample analysis

The $\text{Fe}_3\text{O}_4@\text{THAM-CH}_2\text{CH}_2\text{Cl}$ MNPs adsorbent ability to remove Congo red from environmental water samples was assayed to evaluate the model's

applicability for analysis of actual samples. For this purpose, two samples were treated with the adsorbent. Then each sample, one with a concentration of 15 mg.L^{-1} of Congo red and the other without the addition of Congo red, was individually examined. Congo red removal values ($R\%$, mean \pm standard deviation, $n = 3$) in the tap water and wastewater were $98.48 \pm 1.52\%$ and $98.05 \pm 2.11\%$, respectively.

Table 7 compares the adsorbent of the proposed method and other adsorbents to remove CR. As can be seen, the highest adsorption capacity removal percentage was obtained for the proposed method, proving that the newly developed MNPs, with the advantages of Fe_3O_4

Table 5. Parameters of kinetic models for adsorption process of Congo dye red on the adsorbent.

| Kinetic models Test | Equation | Plot | Parameters | Values |
|---------------------|---|-------------------------------|------------|----------|
| Pseudo-first order | $\log(q_e - q_t) = \log q_e - \frac{k_1}{2.303} t$ | $\log(q_e - q_t)$ against t | k_1 | 0.04053 |
| | | | q_e | 0.365932 |
| | | | R^2 | 0.5583 |
| Pseudo-second order | $\frac{t}{q_t} = \frac{1}{k_2 q_e^2} + \frac{1}{q_e} t$ | t/q_t against t | k_2 | 0.885653 |
| | | | q_e | 5.720824 |
| | | | R^2 | 0.9981 |

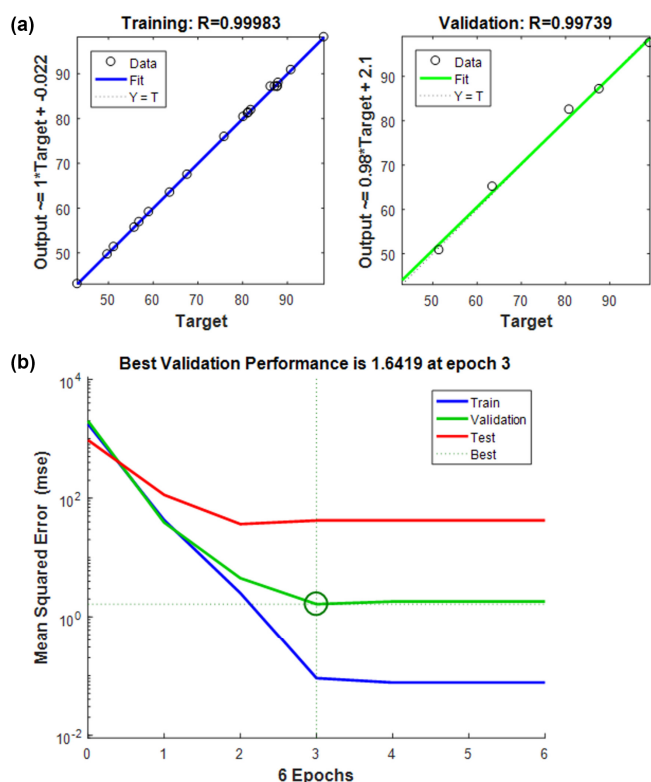


Fig. 4. A relationship between outputs and targets of the ANN model (a), and the MSE versus the number of epochs (b).

MNPs adsorbent combined with THAM, had improved adsorption capacity, stability, and recyclability. Overall, the proposed model designed with an experimental approach (using Taguchi, RSM, and ANN methods) has several advantages. These include a simpler adsorption method, lower cost, shorter analysis time, and more reliable and accurate data. Moreover, combining the Fe_3O_4 MNPs adsorbent with THAM ($\text{Fe}_3\text{O}_4@$ THAM- $\text{CH}_2\text{CH}_2\text{Cl}$ MNPs adsorbent) for removal of CR from the aqueous environment gives the advantages of improved adsorption capacity, stability, and recyclability.

Table 6. Parameters of thermodynamic for adsorption process of dye by the proposed adsorbent.

| Temperature (K) | ΔG° (KJ.mol ⁻¹) | ΔH° (KJ.mol ⁻¹) | ΔS° (KJ.mol ⁻¹ .K ⁻¹) |
|-----------------|--|--|---|
| 293.15 | -51.9347 | -19.6076 | 0.110275 |
| 298.15 | -52.4861 | -19.6076 | 0.110275 |
| 303.15 | -53.0375 | -19.6076 | 0.110275 |
| 308.15 | -53.5889 | -19.6076 | 0.110275 |
| 313.15 | -54.1402 | -19.6076 | 0.110275 |
| 318.15 | -54.6916 | -19.6076 | 0.110275 |
| 323.15 | -55.243 | -19.6076 | 0.110275 |

Table 7. Comparison of adsorbent of proposed method and other adsorbents to remove CR.

| Adsorbent | Adsorption capacity (mg.g ⁻¹) | Ref. |
|--|---|------------|
| $\text{Fe}_3\text{O}_4@$ THAM- $\text{CH}_2\text{CH}_2\text{Cl}$ | 137 | This study |
| $\text{Fe}_3\text{O}_4/\text{Bi}_2\text{O}_3$ | 92.24 | 34 |
| $\text{Fe}_3\text{O}_4@$ TiO ₂ @GO | 89.95 | 35 |
| Fe_3O_4 | 28.46 | 36 |
| $\text{Fe}_3\text{O}_4@$ APTES | 118 | 37 |
| Pd-NP-AC | 126.6 | 38 |
| $\text{Fe}_3\text{O}_4@$ SiO ₂ | 36.2 | 39 |

4. Conclusions

This paper describes a simple and efficient procedure to remove Congo red from sample solutions using $\text{Fe}_3\text{O}_4@$ THAM- $\text{CH}_2\text{CH}_2\text{Cl}$ MNPs as a new adsorbent. The best adsorption efficiency was obtained using 0.04 g of adsorbent, 17 mg.L⁻¹ of dye, pH = 6.6, and ultrasonic treatment for 7.2 min. The model's response level predictions and experimental data collected under optimized conditions were compared. The data indicated the adsorption efficiency of dye in the range of 97.85 - 99.65 %. The larger R^2 for the pseudo-second kinetic model indicates that this model is more suitable to describe the adsorption process of Congo red on the $\text{Fe}_3\text{O}_4@$ THAM- $\text{CH}_2\text{CH}_2\text{Cl}$ MNPs adsorbent. The Langmuir adsorption isotherm had a larger correlation coefficient ($R^2 = 0.9987$), which indicates the best fit with the experimental data and the proposed adsorption process is more suitable for the Congo red adsorption process. According to the results from thermodynamic parameters, the negativity of ΔG° and ΔH° showed that the adsorption process is spontaneous and exothermic. Congo red removal values (R %, mean \pm standard deviation, $n = 3$) in tap water and wastewater were 98.48 ± 1.52 % and 98.05 ± 2.11 %, respectively. The good adsorption efficiency indicates that the model could remove significant amounts of Congo red from the water environment. Modeling by ANN indicated that the R^2 of the graphs are close to one, which shows the validity of the ANN model for the removal of CR dye in successfully predicting the laboratory results of the $\text{Fe}_3\text{O}_4@$ THAM- $\text{CH}_2\text{CH}_2\text{Cl}$ MNPs adsorbent.

Disclosure statement

No potential conflict of interest was reported by the authors.

Acknowledgement

We would like to thank the University of Sistan and Baluchestan for supporting this research.

References

- [1] Kalpana, R., Maheshwaran, M., Vimali, E., Soosai, M.R., Shivamathi, C.S., Moorthy, I.G., Ashokkumar, B. & Varalakshmi, P. (2020). Decolorization of textile dye by halophilic *Eiguobacterium* sp.VK1: Biomass and exopolysaccharide (EPS) enhancement for bioremediation of Malachite Green. *ChemistrySelect*, 5(28) 8787-8797.
- [2] Abdelaziz, M.A., Owda, M.E., Abouzeid, R.E., Alaysuy, O., & Mohamed, E.I. (2022). Kinetics, isotherms, and mechanism of removing cationic and anionic dyes from aqueous solutions using chitosan/magnetite/silver nanoparticles. *Int. J. Biol. Macromol.* 225, 1462-1475.
- [3] Zhou, G., Li, S., Meng, Q., Niu, C., Zhang, X., & Wang, Q. (2023). A new type of highly efficient fir sawdust-based super adsorbent: Remove cationic dyes from wastewater. *Surf. Interf.* 36, 102637.
- [4] Kausor, M.A., & Chakraborty, D. (2020). Optimization of system parameters and kinetic study of photocatalytic degradation of toxic acid blue 25 dye by Ag₃PO₄@ RGO nanocomposite. *J. Nanopart. Res.* 22, 93.
- [5] Cao, M., Shen, Y., Yan, Z., Wei, Q., Jiao, T., Shen, Y., & Yue, T. (2021). Extraction-like removal of organic dyes from polluted water by the graphene oxide/PNIPAM composite system. *Chem. Eng. J.* 405, 126647.
- [6] Teo, S.H., Ng, C.H., Islam, A., Abdulkareem-Alsultan, G., Joseph, C.G., Janaun, J., & Awual, M.R. (2022). Sustainable toxic dyes removal with advanced materials for clean water production: A comprehensive review, *J. Clean. Prod.* 332, 130039.
- [7] Xiong, G., Zhang, Q., Ren, B., You, L., Ding, F., He, Y., & Sun, Y. (2020). Highly efficient and selective adsorption of cationic dyes in aqueous media on microporous hyper crosslinked polymer with abundant and evenly dispersed sulfonic groups. *ChemistrySelect* 5(22) 6541-6548.
- [8] Bhaumik, M., McCrindle, R.I., & Maity, A. (2015). Enhanced adsorptive degradation of Congo red in aqueous solutions using polyaniline/Fe⁰ composite nanofibers. *J. Chem. Eng.* 260, 716-729.
- [9] Tan, Y.J., Sun, L.J., Li, B.T., Zhao, X.H., Yu, T., Ikuno, N., Ishii, K., & Hu, H.Y. (2017). Fouling characteristics and fouling control of reverse osmosis membranes for desalination of dyeing wastewater with high chemical oxygen demand. *Desalination*, 419, 1-7.
- [10] Ouaddari, H., Karim, A., Achiou, B., Saja, S., Aaddane, A., Bennazha, J., El Hassani, I.E.A., Ouammou, M., & Albizane, A. (2019). New low-cost ultrafiltration membrane made from purified natural clays for direct Red 80 dye removal. *J. Environ. Chem. Eng.* 7(4) 103268.
- [11] Li, Y., Li, H., Liu, F., Zhang, G., Xu, Y., Xiao, T., Long, J., Chen, Z., Liao, D., Zhang, J., & Lin, L. (2020). Zero-valent iron-manganese bimetallic nanocomposites catalyze hypochlorite for enhanced thallium(I) oxidation and removal from wastewater: Materials characterization, process optimization and removal mechanisms. *J. Hazard. Mater.* 386, 121900.
- [12] Finkbeiner, P., Moore, G., Pereira, R., Jefferson, B., Jarvis, P. (2020). The combined influence of hydrophobicity, charge and molecular weight on natural organic matter removal by ion exchange and coagulation. *Chemosphere*, 238, 124633.
- [13] Mohaghegh, N., Endo-Kimura, M., Wang, K., Wei, Z., Najafabadi, A.H., Zehtabi, F., & Kowalska, E. (2023). Apatite-coated Ag/AgBr/TiO₂ nanocomposites: Insights into the antimicrobial mechanism in the dark and under visible-light irradiation. *Appl. Surf. Sci.* 617, 156574.
- [14] Agha Beygli, R., Mohaghegh, N., & Rahimi, E. (2019). Metal ion adsorption from wastewater by g-C₃N₄ modified with hydroxyapatite: a case study from Sarcheshmeh Acid Mine Drainage. *Res. Chem. Intermediat.* 45, 2255-2268.
- [15] Choudhary, R., Pandey, O.P., & Brar, L.K. (2022). Novel ultrasonic pretreatment for HTC carbon nanosphere size control without yield compromise. *J. Nanopart. Res.* 24, 75.
- [16] Zirpe, M., & Thakur, J. (2022). Sono-assisted synthesis of AgFeO₂ nanoparticles for efficient removal of Basic Green-4 dye from aqueous solution.

- J. Nanopart. Res.* 24, 240.
- [17] Rahmani, M., Kaykhahi, M., & Sasani, M. (2018). Application of Taguchi L16 design method for comparative study of ability of 3A zeolite in removal of Rhodamine B and Malachite green from environmental water samples. *Spectrochim. Acta A*, 188, 164-169.
- [18] Shojaei, S., Shojaei, S., & Pirkamali, M. (2019). Application of Box–Behnken design approach for removal of acid black 26 from aqueous solution using zeolite: Modeling, optimization, and study of interactive variables. *Water Conserv. Sci. Eng.* 4(1) 13-19.
- [19] Pourabadeh, A., Baharinikoo, L., Shojaei, S., Mehdizadeh, B., Davoodabadi Farahani, M. & Shojaei, S. (2020). Experimental design and modelling of removal of dyes using nano-zero-valent iron: a simultaneous model. *Int. J. Environ. An. Ch.* 100(15) 1707-1719.
- [20] Rahimi, E., & Mohaghegh, N. (2017). New hybrid nanocomposite of copper terephthalate MOF-graphene oxide: synthesis, characterization and application as adsorbents for toxic metal ion removal from Sungun acid mine drainage. *Environ. Sci. Pollut. R.* 24(28) 22353-22360.
- [21] Samimi, M., & Shahriari-Moghadam, M. (2021). Isolation and identification of *Delftia lacustris* Strain-MS3 as a novel and efficient adsorbent for lead biosorption: Kinetics and thermodynamic studies, optimization of operating variables. *Biochem. Eng. J.* 173, 108091.
- [22] Shojaei, S., Rahmani, M., Khajeh, M., & Abbasian, A.R. (2023). Ultrasound assisted based solid phase extraction for the preconcentration and spectrophotometric determination of malachite green and methylene blue in water samples. *Arab. J. Chem.* 16(8) 104868.
- [23] Guo, Q., Liu, Y., & Qi, G. (2019). Application of high-gravity technology NaOH-modified activated carbon in rotating packed bed (RPB) to adsorb toluene. *J. Nanopart. Res.* 21, 175.
- [24] Samimi, M., & Safari, M. (2022). TMU-24 (Zn-based MOF) as an advance and recyclable adsorbent for the efficient removal of eosin B: Characterization, equilibrium, and thermodynamic studies. *Environ. Prog. Sustain.* 41(5) e13859.
- [25] Faroughi Niya, H., Hazeri, N., Fatahpour, M., & Maghsoodlou, M.T. (2020). Fe₃O₄@THAM-piperazine: a novel and highly reusable nanocatalyst for one-pot synthesis of 1,8-dioxo-octahydro-xanthenes and benzopyrans. *Res. Chem. Intermediat.* 46, 3651-3666.
- [26] Kaur, G., Jayasundara, J.M.R.V., Singh, G., Pawan, Singh, H., & Singh, J. (2023). Photocatalytic dye degradation by recyclable Zn-Co magnetic ferrites at ambient conditions. *Int. J. Environ. An. Ch.*, DOI: 10.1080/03067319.2022.2161900.
- [27] Mirzaei, F. Mohammadi Nilash, M., Sepahvand, H., Fakhari, A.R., & Shaabani, A. (2020). Magnetic solid-phase extraction based on fluconazole-functionalized Fe₃O₄@SiO₂ nanoparticles for the spectrophotometric determination of cationic dyes in environmental water samples. *J. Iran. Chem. Soc.* 17(7) 1591-1600.
- [28] Shojaei, S., Rahmani, M., Khajeh, M., & Abbasian, A.R. (2021). Magnetic-nanoparticle-based dispersive micro-solid phase extraction for the determination of crystal violet in environmental water samples. *ChemistrySelect* 6(19) 4782-4790.
- [29] Khajeh, M., Sarafraz-Yazdi, A., & Fakhri Moghadam, A. (2017). Modeling of solid-phase tea waste extraction for the removal of manganese and cobalt from water samples by using PSO-artificial neural network and response surface methodology. *Arab. J. Chem.* 10(Suppl. 2) S1663-S1673.
- [30] Kaladgi, A.R., Afzal, A., Muthu Manokar, A., Thakur, D., Agbulut, U., Alshahrani, S., Ahmad Saleh, C., & Subbiah, R. (2021). Integrated Taguchi-GRA-RSM optimization and ANN modelling of thermal performance of zinc oxide nanofluids in an automobile radiator. *Case Stud. Therm. Eng.* 26, 101068.
- [31] Hammoudi, A., Moussaceb, K., Belebchouche, C., & Dahmoune, F. (2019). Comparison of artificial neural network (ANN) and response surface methodology (RSM) prediction in compressive strength of recycled concrete aggregates. *Constr. Build. Mater.* 209, 425-436.
- [32] Samimi, M., & Moeini, S. (2020). Optimization of the Ba²⁺ uptake in the formation process of hydrogels using central composite design: Kinetics and thermodynamic studies of malachite green removal by Ba-alginate particles. *J. Particle Sci. Technol.* 6(2) 95-102.
- [33] Samimi, M., & Mohadesi, M. (2023). Size estimation of biopolymeric beads produced by electrospray method using artificial neural network.

- Particul. Sci. Technol.* 41(3) 371-377.
- [34] Zhu, H., Jiang, R., Li, J., Fu, Y., Jiang, S., & Yao, J. (2017). Magnetically recyclable $\text{Fe}_3\text{O}_4/\text{Bi}_2\text{S}_3$ microspheres for effective removal of Congo red dye by simultaneous adsorption and photocatalytic regeneration. *Sep. Purif. Technol.* 179, 184-193.
- [35] Li, L., Li, X., Duan, H., Wang, X., & Luo, C. (2014). Removal of Congo Red by magnetic mesoporous titanium dioxide–graphene oxide core–shell microspheres for water purification. *Dalton T.* 43(22) 8431-8438.
- [36] Mou, Y., Yang, H., & Xu, Z. (2017). Morphology, surface layer evolution, and structure–dye adsorption relationship of porous Fe_3O_4 MNPs prepared by solvothermal/gas generation process. *ACS Sustain. Chem. Eng.* 5(3) 2339-2349.
- [37] Yan, T.G., Wang, L.J. (2014). Adsorption of C.I. Reactive Red 228 and Congo Red dye from aqueous solution by amino-functionalized Fe_3O_4 particles: Kinetics, equilibrium, and thermodynamics. *Water Sci. Technol.* 69(3) 612-621.
- [38] Ahmadi, K., Ghaedi, M., & Ansari, A. (2015). Comparison of nickel doped zinc sulfide and/or palladium nanoparticle loaded on activated carbon as efficient adsorbents for kinetic and equilibrium study of removal of Congo red dye. *Spectrochim. Acta A*, 136, 1441-1449.
- [39] Wang, P., Wang, X., Yu, S., Zou, Y., Wang, J., Chen, Z., & Wang, X. (2016). Silica coated Fe_3O_4 magnetic nanospheres for high removal of organic pollutants from wastewater. *Chem. Eng. J.* 306, 280-288.

Additional information

Correspondence and requests for materials should be addressed to M. Rahmani.

HOW TO CITE THIS ARTICLE

Mokari, R.; Rahmani, M. (2022). Application of $\text{Fe}_3\text{O}_4@\text{THAM-CH}_2\text{CH}_2\text{Cl}$ magnetic nanoparticle as a new adsorbent in ultrasonically assisted removal of Congo red from aqueous solutions. *J. Particle Sci. Technol.* 8(2) 103-114.

DOI: [10.22104/JPST.2023.6153.1223](https://doi.org/10.22104/JPST.2023.6153.1223)

URL: https://jpst.irost.ir/article_1270.html